UNDERSTANDING THE ASYMPTOTIC PERFORMANCE OF MODEL-BASED RL METHODS

William F. Whitney and Rob Fergus
Department of Computer Science
New York University
New York, NY 10011, USA
{wwhitney,fergus}@cs.nyu.edu

ABSTRACT

In complex simulated environments, model-based reinforcement learning methods typically lag the asymptotic performance of model-free approaches. This paper uses two MuJoCo environments to understand this gap through a series of ablation experiments designed to separate the contributions of the dynamics model and planner. These reveal the importance of long planning horizons, beyond those typically used. A dynamics model that directly predicts distant states, based on current state and a long sequence of actions, is introduced. This avoids the need for many recursions during long-range planning, and thus is able to yield more accurate state estimates. These accurate predictions allow us to uncover the relationship between model accuracy and performance, and translate to higher task reward that matches or exceeds current state-of-the-art model-free approaches.

1 INTRODUCTION

Model-based reinforcement learning (MBRL) has many potential benefits over model-free approaches. These include (i) the ability to generalize to new tasks in the environment, without having to retrain; (ii) learning from off-policy data and (iii) sample efficiency. However, in simulated environments where data is plentiful, model-based approaches struggle to approach the asymptotic performance of model-free methods Nagabandi et al. (2017); Pong et al. (2018); Chua et al. (2018). Several possible explanations present themselves: the planner used for selecting optimal actions under the model might be insufficiently powerful; the model might not be able to accurately model the dynamics; or the planning horizon might not be long enough.

This paper address these questions by teasing apart the different factors involved in an MBRL framework, applied to two deterministic MuJoCo environments (Todorov et al., 2012), with the aim of understanding the gap in asymptotic performance with respect to model-free approaches. In particular, we demonstrate that bias caused by short planning horizons and poor accuracy of long-term predictions is the cause of the poor performance of existing MBRL methods in the unlimited-sample regime. Our experiments show that, with a perfect dynamics model, the optimal planing horizon can be over 100 steps – much longer than typically considered in many MBRL approaches. Correspondingly, the performance is typically limited by the ability of the model to accurately predict over long-time scales, not just a few time-steps.

Existing approaches to MBRL rely on a single-step dynamics model that predict the next state, given the current state and an action. As can be see in Figure 5, over long time-horizons the errors compound due to recursive application of the model, yielding inaccurate state estimates which are not useful for planning. Instead, we propose an alternate form of dynamics model that takes as input a *sequence* of actions along with the current state and directly predicts many time-steps into the future. This approach provides accurate prediction over long time horizons, allowing us to uncover the relationship between model accuracy and performance. This reveals that MBRL with sufficiently good learned models matches or exceeds the performance of state-of-the-art model-free methods.

1.1 Related Work

Non-Parametric Model-Based RL: Gaussian processes are popular approach to modeling non-linear dynamics due to their low sample complexity and their ability to explicitly represent epistemic uncertainty. Consequently, numerous MBRL approaches use them, e.g. Kocijan et al. (2004); Ko et al. (2007); Grancharova et al. (2008); Deisenroth & Rasmussen (2011); Deisenroth et al. (2014). However via the choice of kernel they impose potentially unrealistic smoothness constraints and do not scale to large data settings, limiting their asymptotic performance in practice.

Combining model-based and model-free methods: Due to the sample efficiency of model-based methods and superior asymptotic performance of model-free methods, several works have proposed to learn dynamics models using a few trajectory samples, then use those models to train or augment a model-free policy. The classic Dyna algorithm (Sutton, 1990) uses a model to extend Bellman updates multiple steps. Deisenroth & Rasmussen (2011) learns a Gaussian process model of the dynamics function and uses it to train an RBF network policy, and Gal et al. (2016) enables the model to scale to larger data by using Bayesian neural networks in place of GPs. Levine et al. (2016) fits a time-varying locally linear model around a trajectory, then trains a neural network policy to follow trajectories found by iLQR (Todorov & Li, 2005). Silver et al. (2016) learns an implicit model of the dynamics for implicit planning via value estimation; in an inversion of this technique, Pong et al. (2018) learn an explicit model of Q values for explicit planning via constrained optimization. Weber et al. (2017) learns a neural network dynamics model which is unrolled inside a policy to inform an actor-critic agent. Nagabandi et al. (2017) trains a neural network dynamics model on control tasks and uses it to take actions, then uses that model-based policy to speed the training of a model-free policy via imitation learning. These works largely seek to either (i) augment a model-free method with a model for faster learning, or (ii) make up for the asymptotic deficiencies of a model-based method by transitioning to model-free. In this work we instead directly investigate the causes of MBRL's poor asymptotic performance with the aim of making a transition to model-free unnecessary.

MBRL with neural network models: The idea of using neural networks to enable model-based control of nonlinear systems goes back decades (Miller et al., 1990; Schmidhuber, 1990; Hunt et al., 1992; Bekey & Goldberg, 2012; Draeger et al., 1995), but until recently has only seen significant success on systems with relatively simple dynamics. Several works have endeavored to use neural network generative models of images for model-based control (Wahlström et al., 2015; Watter et al., 2015; Finn & Levine, 2017); these policies have typically used short planning horizons and struggled to equal model-free performance on complex tasks. Lenz et al. (2015) learn recurrent neural network dynamics models, then use backpropagation through time to select actions and control a robotic arm, and Henaff et al. (2017) extend this concept to both discrete and continuous action spaces. Clavera et al. (2018) combine meta-learning with MBRL using neural network models to rapidly adapt to novel environments. Srinivas et al. (2018) uses imitation learning to train a model to plan by gradient descent, which relies on an existing expert rather than learning from scratch.

The closest work to ours is Chua et al. (2018). This follows a similar recipe, with similar planning and constructing a dataset online, but with different models and different goals. We use deterministic neural networks which predict many steps into the future to understand the impact of model- and horizon-bias on asymptotic performance of MBRL methods on long-horizon problems. Chua et al. (2018) uses a bootstrapped ensemble of probabilistic neural networks to improve the performance of MBRL in the few-sample regime. While that work achieves strong performance on short-horizon tasks, in our experiments we find it struggles to equal model-free methods on tasks with very long horizons.

2 Approach

In this section we describe the models used in our experiments, the action-conditional predictor (ACP) and the novel plan-conditional predictor (PCP), which predicts the outcome of a sequence of actions with a single model step. We then detail the framework we use for planning with and training these models.

2.1 NOTATION

We denote states and actions at a time t by s_t and a_t. In the environments we consider, both s_t and a_t are continuous vectors. We use H to refer to the planning horizon of an MPC policy. We refer to a sequence of actions as a *plan*; a plan constructed with horizon H is thus $p = \{a_1, ..., a_H\}$. In a set of plans $\{p^1, ..., p^n\}$, a^i_j refers to the jth action of the ith plan.

We consider models which predict a future state given the current state and one or more actions. We denote R to be the *range* of such a model, which is the number of steps this model predicts in a single application: $f_R(s_t, a_t, \ldots, a_{t+R-1}; \theta) = \tilde{s}_{t+R}$, for parameters θ.

We apply the model recursively using the notation $F_T(s_t, a_t, \ldots, a_{T-1}; \theta) = f_R(\ldots f_R(f_R(s_t, a_t, \ldots, a_{t+R-1}; \theta), a_{t+R}, \ldots, a_{t+2R-1}; \theta) \ldots, a_{T-R}, \ldots, a_{T-1}; \theta) = \tilde{s}_T$. That is, $F_T()$ applies $f_R()$ recursively T/R times.

2.2 PLAN-CONDITIONAL PREDICTORS

To test our conjecture that compounding errors limit the asymptotic performance of existing models on long-horizon RL tasks, we propose plan-conditional predictors (PCPs). A PCP takes the form $f_R(s_t, a_t, \ldots, a_{t+R-1}) = \tilde{s}_{t+R}$ for some range $R > 1$. If $R = 1$, then it reduces to the standard approach (Deisenroth & Rasmussen, 2011; Gal et al., 2016; Henaff et al., 2017; Nagabandi et al., 2017; Chua et al., 2018) which predicts only a single time-step at a time, and which we call an action-conditional predictor (ACP). As shown in Figure 1, a PCP can predict H steps into the future using H/R recursive applications of the model instead of H applications required by an action-conditional predictor.

(a) Action-conditional predictors must recurse H times to make a prediction H steps into the future.

(b) A plan-conditional predictor with range R only needs to recurse H/R times (shown here as twice).

Figure 1: Action-conditional vs. plan-conditional predictors.

For visualization purposes, in some experiments we use a variant of a plan-conditional predictor which takes as input a state and a variable number of actions R' where $1 \leq R' \leq R$, the remainder of action inputs being set to zero. This allows us to plot error or render video of the PCP's predictions at each intermediate timestep instead of only at multiples of R.

There are many possible parameterizations that could be used in a PCP. In this work we choose deep fully-connected neural networks. There are several reasons for this: (i) the space of inputs grows exponentially with the range R, thus models with high capacity are needed to minimize model bias; (ii) since the goal is to understand asymptotic performance, a large data regime is assumed and sample complexity is a secondary issue. While a range of other architectures might provide a more efficient parameterization, e.g. RNNs, exploration of these is orthogonal to our investigation. For both `Swimmer` and `HalfCheetah`, the ACP and PCP networks consist of fully-connected networks with 9 hidden layers with 1000 units each using the SELU activation function (Klambauer et al., 2017). The input state and action(s) are concatenated before being used as input to the network.

The same loss function is used for training PCPs and ACPs, namely $\|\tilde{s}_{t+R} - s_{t+R}\|_2^2$, where s is the raw MuJoCo state. We assume that the environment forms a Markov decision process (MDP) (Bellman, 1957) with deterministic dynamics, properties shared by the tasks considered in this work. These assumptions allow us to focus exclusively on the significance of model fidelity and planning horizon to MBRL, but removing them is an interesting direction for future work.

2.3 SELECTING OPTIMAL ACTIONS

In order to turn a predictor into a policy, we employ an off-the-shelf planning approach, namely the cross-entropy method (CEM) (Botev, 2011), to find a plan that is optimal up to some horizon H. We take the first action from that plan and then replan, a technique known as model-predictive control (MPC) or receding-horizon control (Mayne & Michalska, 1990).

2.3.1 PLANNING WITH CROSS-ENTROPY METHOD

Given a predictor F, a horizon H, and a reward function r, we would like to find an optimal plan:

$$p_t^* = \underset{a_t,\ldots,a_{t+H-1}}{\arg\max} \sum_{i=0}^{H-1} r(\tilde{s}_{t+i}, a_{t+i}) \;\mid\; \tilde{s}_{t+i} = F_H(s_t, a_t, \ldots, a_{t+i-1})$$

For both MuJoCo environments, the reward function is dominated by the distance traveled in the x-dimension[1]. Thus we need only consider reward at the end of the planning horizon $r(s_{t+H})$ and not the exact path traversed. This reduces the form of the optimal plan under a predictor F to

$$p_t^* = \underset{a_t,\ldots,a_{t+H-1}}{\arg\max} \; r(F_H(s_t, a_t, \ldots, a_{t+H-1}))$$

The cross-entropy method starts with a set of plans p drawn from a candidate distribution C. In continuous control tasks, sampling actions independently along a trajectory results in near-zero net motion. Therefore it is common to instead use correlated action noise for exploration or trajectory sampling, e.g. an Ornstein-Uhlenbeck process (Uhlenbeck & Ornstein, 1930) as in DDPG (Lillicrap et al., 2015). We define the candidate $C(\cdot)$ distribution by the following sampling process:

$$a_0 \sim \mathcal{U}(-1, 1)$$
$$a_{t+1} = \min(\max(\mathcal{N}(\mu = a_t, \sigma = 0.2), -1), 1)$$

i.e. the sampled actions are clamped to be in the range ± 1 which are the limits of the action space.

The overall planning framework is shown in Figure 2. After drawing an initial set of N plans $\{p^1, \ldots, p^N\} \sim C(\cdot)$, these are passed through the predictor F to estimate rewards $r^1, \ldots, r^N$, which are used to rank the plans. The top K are then passed to a 2nd round (red box). Additionally, their mean and variance are computed[2] and used as parameters for a Gaussian distribution from which $N - K$ new plans are sampled (green box). The combined set of plans are then passed to the PCP to rank them. The output from the planner is the first action from the top-ranked plan (yellow box) at the final planning round, which is executed by the agent in the environment.

The top K trajectories from the final round are used to seed the initial set of plans for replanning at the next timestep, after clipping the first action from each. In practice, we use 3 rounds of planning at each timestep, i.e. two rounds of resampling (the figure omits the 3rd round for clarity). In our experiments, we use $N = 50$ and $K = 5$.

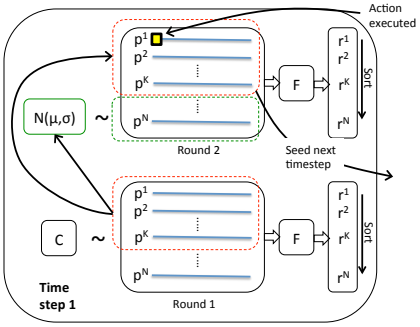

Figure 2: Our off-the-shelf planner, based on the cross-entropy method (Botev, 2011). See text for details.

Algorithm 1 On-policy data aggregation and training

Initialize dataset $\mathbb{D}$ with trajectories from random policy
while not converged **do**
  $\theta \leftarrow \arg\min_\Theta \mathbb{E}_{s_t, a_{t\ldots t+R-1}, s_{t+R} \sim \mathbb{D}} \left(f_R(s_t, a_{t\ldots t+R-1}) - s_{t+R}\right)^2$
  for $m = 0 \ldots M$ **do**
    for $t = 0 \ldots T$ **do**
      $s_t \leftarrow$ Env.get_observation()
      $p_t \leftarrow \arg\max_{a_{t\ldots t+H-1}} r(F_H(s_t, a_{t\ldots t+H-1}; \theta))$
      $a_t \leftarrow \text{head}(p_t)$
      Env.execute(a_t).
    end for
    $\mathbb{D} \leftarrow \mathbb{D} \bigcup (s_{0\ldots T}, a_{0\ldots T-1})$
  end for
end while

[1] In all experiments we *evaluate* a policy using the original reward function from OpenAI Gym. This simplified reward function is exclusively used inside the policy. We found in experiments using the ground-truth dynamics as a model that planning with the true reward function instead made no significant difference on these tasks.

[2] Independently at each timestep and action dimension; $\mu(p^1, \ldots, p^n) = \left\{\frac{1}{n}\sum_i a_j^i \mid j \in H\right\}$ and $\sigma(p^1, \ldots, p^n) = \left\{\sqrt{\frac{1}{n}\sum_i \left(a_j^i - \mu(a_j^{1\ldots n})\right)^2} \mid j \in H\right\}$.

2.4 ONLINE TRAINING

The planning framework described above turns the PCP model into a policy which outputs an action at each time step. To train this policy, the underlying PCP model must be updated in an online fashion.

This requires a dataset of trajectories $\{s_{0...T}, a_{0...T-1}\}$ that covers the environment's state-action space. We follow Nagabandi et al. (2017); Chua et al. (2018) and others and collect this dataset by alternating between fitting the model to the existing data and using our planning procedure (2.3.1) to generate more trajectories from the environment. We collect trajectories from the environment for $M = 100$ episodes. These trajectories are added to the training set and the PCP model is updated with SGD for 10 epochs using AMSGrad (Reddi et al., 2018). The overall procedure is detailed in Algorithm 1 and is essentially the standard template for MBRL (Deisenroth & Rasmussen, 2011; Gal et al., 2016; Nagabandi et al., 2017; Chua et al., 2018).

3 EXPERIMENTS

3.1 EFFECT OF PLANNING HORIZON AND MODEL RANGE

In this experiment we directly test our hypothesis that plan-conditional predictors are able to benefit from longer planning horizons than action-conditional predictors. Figure 3 shows that while an ACP model is competitive for planning horizons up to 20 timesteps, its performance falls substantially below the PCP models by 40 timesteps. The ACP model scores best at a horizon of 60 timesteps; beyond that its performance degrades as its predictions become unusably inaccurate.

By contrast the PCP models shown, which need only be recursively applied between 3 and 20 times, all show monotonically increasing rewards as the planning horizon is increased. This reveals two things: the `Swimmer` task has a minimum optimal planning horizon of at least 100 timesteps, and the PCP models are able to predict with sufficient accuracy to be useful even over that long horizon.

In the next experiments we tease apart the different factors of planning horizon, range, and accuracy that combine to produce these results.

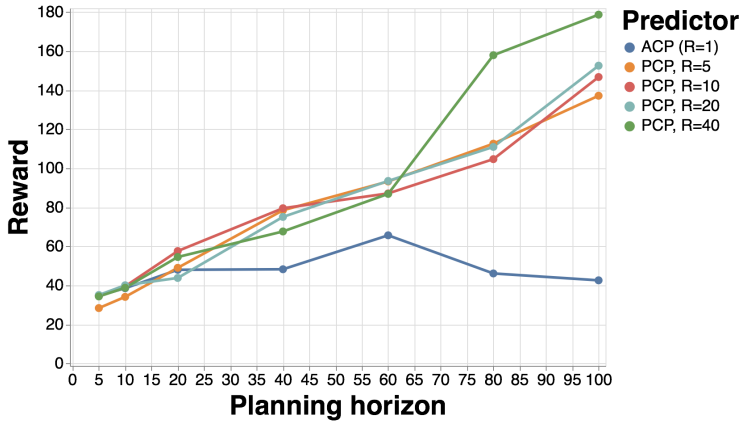

Figure 3: Reward attained at convergence on `Swimmer` by action-conditional predictors (Range $=$ 1) and plan-conditional predictors (Range $>$ 1) trained using different planning horizons. For this experiment we use the PCP variant which can make intermediate predictions to allow planning horizons that are not even multiples of ranges, e.g. a range 40 model with horizon 60.

3.2 PLANNING HORIZON VS REWARD

Using a ground-truth model of the environment (that is, MuJoCo itself) in conjunction with our planner we can look at performance as a function of planning horizon for these tasks. That is, we define a new predictor MJC$(s_t, a_{t...t+T})$ which can make predictions arbitrarily far into the future. This predictor works internally by creating a new copy `env_internal` of the Gym environment. To make

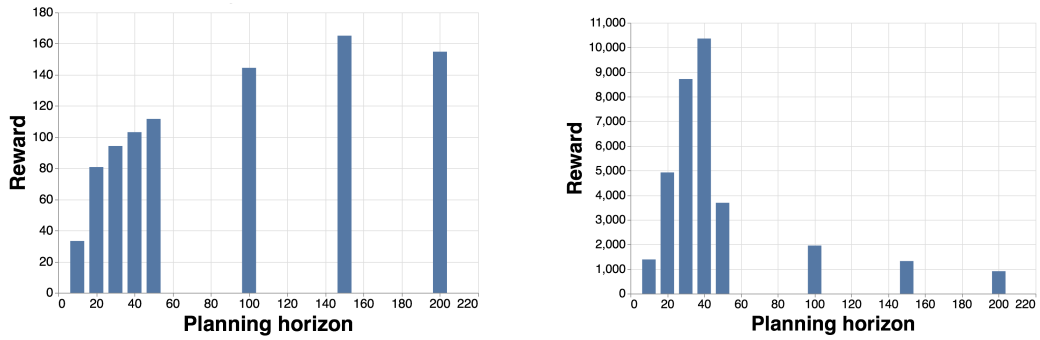

(a) `Swimmer` (b) `HalfCheetah`

Figure 4: Reward as a function of planning horizon for `Swimmer` and `HalfCheetah` using ground-truth dynamics with our planner. `Swimmer` performance increases up to a horizon of $H = 150$. For `HalfCheetah` the optimal horizon is around $H = 40$, after which performance decreases due to the instability of the simulation when using single- instead of double-precision floating point.[3]

a prediction MJC$(s_t, a_{t...t+T}) = s_{t+1}$, this predictor will call `env_internal.set_state`(s_t), then repeatedly call `env_internal.step`(a_{t+i}) for $i = 0...T$. Its output is the observation after the final action has been executed. This ground-truth predictor can be used for planning like any other.

The results of this experiment, shown in Figure 4, show that the optimal planning horizons for `Swimmer` and `HalfCheetah` are at around 150 and 40 timesteps, respectively. These results provide additional clarity to those presented in the previous experiment. Policies that use the ground-truth dynamics as their predictor perform better as the horizon increases due to the decreased bias of the long-horizon reward estimate. The approximate dynamics model from PCPs show similar gains. However, beyond a certain planning horizon the quasi-random search in the planner becomes less effective due to variance caused by the huge size of the search space, causing the reward to dip for $H > 150$.

Previous work (Nagabandi et al., 2017; Chua et al., 2018) has demonstrated planning for 20 or 30 timesteps with a neural network dynamics model (and in particular, the recent Chua et al. (2018) achieves impressive scores on HalfCheetah). However, to our knowledge planning horizons above 50 timesteps remain untested. This leads us to investigate the accuracy at very long range prediction of traditional action-conditional predictors as well as our plan-conditional predictors.

3.3 Model Range vs Accuracy

With the evidence from Section 3.2 that some tasks require planning horizons up to 150 timesteps, we now evaluate action-conditional and plan-conditional predictors on their ability to make long-range predictions in MuJoCo. To enable direct comparisons, we employ a fixed dataset of trajectories from the environment. We generate this dataset by training a model-free PPO (Schulman et al., 2017) agent on `Swimmer` and recording the trajectories that it takes. This ensures that the dataset contains trajectories that involve interacting with the environment in nontrivial ways. We then split that data into a training set and a validation set and train an ACP and a PCP ($R = 50$) to convergence on the training set.

Figure 5 shows the results of evaluating these models on the validation set. While the ACP is able to make extremely accurate predictions a few steps into the future, it suffers from accumulating error when it is recursively applied many times. This suggests an explanation for the inability of the ACP models to take advantage of planning horizons longer than 60 timesteps, as discussed in Section 3.1. As the horizon increases the predictions from an ACP diverge from reality, while simultaneously the

[3]We found it necessary to handicap the ground-truth model on `HalfCheetah` by adding noise to its actions during planning to prevent the planner from breaking the simulation. Without this handicap the planner was able to find nonphysical strategies and achieves expected reward of up to 150,000.

bias from using a too-short planning horizon decreases. This produces an optimal planning horizon of intermediate length given a model with error that increases as a function of depth.

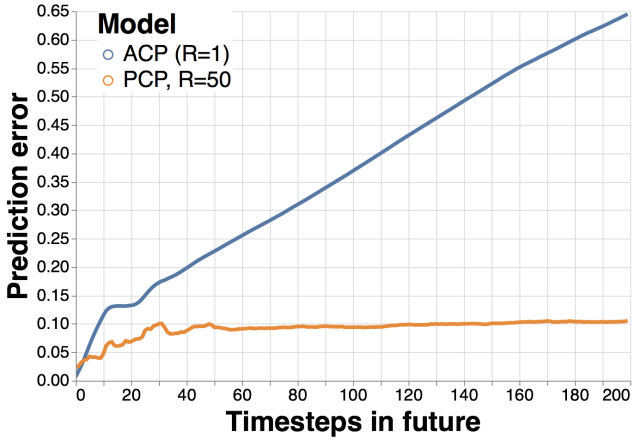

Figure 5: Mujoco `Swimmer` task. Prediction error in estimated distance traveled as a function of timesteps in the future for two models trained on the same dataset of off-line trajectories: a 1-step predictor (blue) and a 50-step predictor (orange). Recursive application of the 1-step model causes the error to grow much faster than the 50-step model. Since the 50-step model only needs four recursive steps error grows slowly.

3.4 Model Accuracy vs Reward

Figure 6 shows the reward vs prediction error for 10 models at various points during online training in the `Swimmer` environment. These results show a clear relationship between low prediction error of the model and high reward, reinforce the importance of having a highly accurate long-range model of the environment. Taken together with the high error for ACPs in Figure 5, this explains that the RL performance of action-conditional predictors is limited by their inability to make accurate predictions at long timescales.

The left panel of Figure 6 shows a very vertical trend at the far left of the plot. We hypothesize that this is due to the changing distribution of the training data as a function of the predictor's accuracy; once a predictor is making accurate predictions, the trajectories that it follows change from being nearly random to more focused. This then means that most of the progress late in training is on refining the predictions on a very narrow distribution of trajectories. These refinements continue to improve the RL performance of the predictor but have little impact on its accuracy along trajectories coming from a different policy.

3.5 Comparison to Other Approaches

In this experiment we evaluate the performance of ACP and PCP models compared to previous reinforcement learning methods, both model-free and model-based, on `Swimmer-v2` and `HalfCheetah-v2` from OpenAI Gym (Brockman et al., 2016)[4].

Our main model-based baseline is PETS (Chua et al., 2018), a state of the art probabilistic neural network-based MBRL algorithm which has been shown to equal or exceed model-free performance on short-horizon tasks. Similar to this work, PETS uses MPC and CEM for model-based control and aggregates a dataset online. On `HalfCheetah` we also compare with the model-based results from Nagabandi et al. (2017), which follows the same basic formula as our work but uses random shooting to find optimal plans instead of CEM. Our model-free baseline is PPO (Schulman et al., 2017) as implemented by Kostrikov (2018), a high-performing actor-critic method.

For each method we run five seeds and allow the algorithm to run to convergence, as we are interested in evaluating asymptotic performance. We train PPO for 100,000 trajectories. On `Swimmer` and

[4]We selected `Swimmer` and `HalfCheetah` to follow the main experiments from Nagabandi et al. (2017).

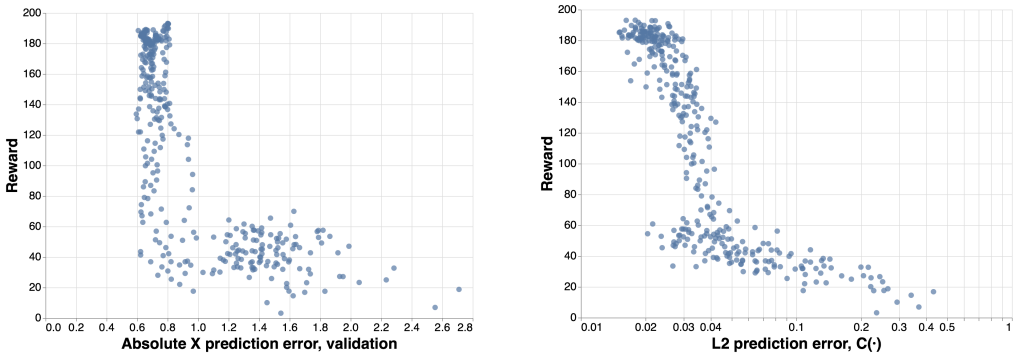

Figure 6: Experiments on `Swimmer` showing the relationship between the predictor's accuracy at $H = 100$ steps into the future and the reward obtained by using that predictor for MPC with a horizon of H timesteps. These plots include five seeds each of ACP and PCP ($R = 50$), with each point representing a particular predictor at some point in the training process. **Left**: Absolute error at predicting the X-coordinate H steps in the future along a trajectory taken by a trained PPO agent. Our policies select actions based on which plan results in the greatest X-coordinate prediction. **Right**: ℓ_2 loss at predicting the outcome from following a plan sampled from the candidate distribution C.

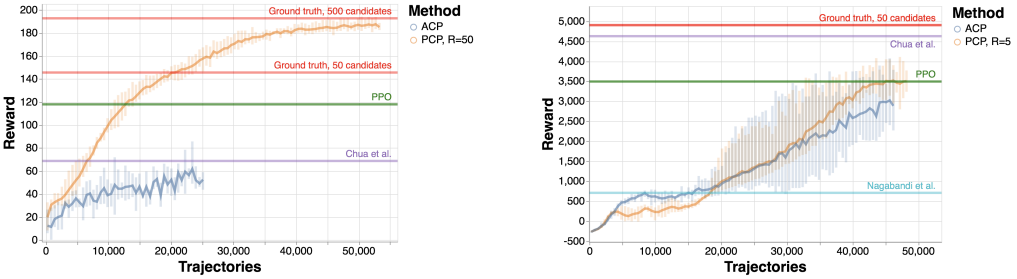

(a) `Swimmer-v2` (b) `HalfCheetah-v2`

Figure 7: These plots show the scores achieved by ACP, PCP, and methods previously published in the literature. Solid lines indicate average reward; translucent bars indicate the best and the worst performance across 5 seeds. **Left**: On `Swimmer` PCP achieves rewards of 185, outperforming any previous model-based or model-free method. In particular, the next-best model-based approach reaches scores less than half those attained by PCP. **Right**: On `HalfCheetah` PCP equals the rewards attained by PPO. PCP outperforms ACP and Nagabandi et al. (2017) despite the planning horizon being a short $H = 20$.

`HalfCheetah` we use planning horizons of 100 and 20 timesteps respectively for the ACP, PCP, and PETS results. For each of the baseline methods we plot a horizontal line indicating the best score achieved by that method at any point in training, after averaging over the random seeds and over several consecutive episodes. We also show lines for the score achieved by using the ground-truth dynamics with the same planner as we use for PCP. In the case of Nagabandi et al. (2017) the score shown is that reported in their work; while the version of the `HalfCheetah` environment that they use is slightly different from the Gym one, we believe the numbers to be roughly comparable.

Figure 7 shows the results of this experiment. On `Swimmer`, which has a very long planning horizon, PCP achieves rewards more than 50% higher than the next-best method, while on `HalfCheetah` it equals the performance of PPO. We speculate that the extremely high rewards achieved by Chua et al. (2018) on `HalfCheetah` are due in part to the difference in settings for CEM betweeen our two works; while we use 3 steps of CEM optimization with 50 candidates per step, Chua et al. (2018) use 5 steps of optimization on 500 candidates.

4 DISCUSSION

In this work we considered the problem of model bias in model-based reinforcement learning. In the largely deterministic environments considered, we show that optimal planning horizons can be large, beyond 100 timesteps. Over these horizons, existing NN-based models do not perform well. We propose more robust alternatives. Further experiments confirm that model accuracy is crucial to end task performance.

Our experiments make several simplifying assumptions, most notably the availability of unlimited samples and deterministic environment dynamics. Sample complexity would undoubtedly be improved by replacing the current overparameterized MLP architecture with something more efficient, an interesting future direction. Another important area for future work is understanding the interaction of long-range planning with stochasticity in the environment, including the development of generative models capable of predictions over long horizons.

REFERENCES

George A Bekey and Kenneth Y Goldberg. *Neural Networks in robotics*, volume 202. Springer Science & Business Media, 2012.

Richard Bellman. A Markovian decision process. *Journal of Mathematics and Mechanics*, pp. 679–684, 1957.

Zdravko I. Botev. The cross-entropy method for optimization. 2011.

Greg Brockman, Vicki Cheung, Ludwig Pettersson, Jonas Schneider, John Schulman, Jie Tang, and Wojciech Zaremba. Openai gym. *CoRR*, abs/1606.01540, 2016.

Kurtland Chua, Roberto Calandra, Rowan McAllister, and Sergey Levine. Deep reinforcement learning in a handful of trials using probabilistic dynamics models. *arXiv preprint arXiv:1805.12114*, 2018.

I. Clavera, A. Nagabandi, R. S. Fearing, P. Abbeel, S. Levine, and C. Finn. Learning to adapt: Meta-learning for model-based control. *arXiv 1803.11347*, 2018.

M. Deisenroth, D. Fox, and C. E. Rasmussen. Gaussian processes for data-efficient learning in robotics and control. *IEEE Transactions on Pattern Analysis and Machine Intelligence (PAMI)*, (2):408423, 2014.

Marc Peter Deisenroth and Carl E. Rasmussen. PILCO: A model-based and data-efficient approach to policy search. In *ICML*, 2011.

Andreas Draeger, Sebastian Engell, and Horst Ranke. Model predictive control using neural networks. *IEEE Control systems*, 15(5):61–66, 1995.

Chelsea Finn and Sergey Levine. Deep visual foresight for planning robot motion. *2017 IEEE International Conference on Robotics and Automation (ICRA)*, pp. 2786–2793, 2017.

Yarin Gal, Rowan McAllister, and Carl Edward Rasmussen. Improving pilco with bayesian neural network dynamics models. In *Data-Efficient Machine Learning workshop, ICML*, 2016.

A. Grancharova, J. Kocijan, and T. A. Johansen. Explicit stochastic predictive control of combustion plants based on gaussian process models. *Automatica*, 44(6):1621–1631, 2008.

Mikael Henaff, William F Whitney, and Yann LeCun. Model-based planning with discrete and continuous actions. *arXiv preprint arXiv:1705.07177*, 2017.

K Jetal Hunt, D Sbarbaro, R Żbikowski, and Peter J Gawthrop. Neural networks for control systemsa survey. *Automatica*, 28(6):1083–1112, 1992.

Günter Klambauer, Thomas Unterthiner, Andreas Mayr, and Sepp Hochreiter. Self-normalizing neural networks. In *Advances in Neural Information Processing Systems*, pp. 971–980, 2017.

J. Ko, D. J. Klein, D. Fox, and D. Haehnel. Gaussian processes and reinforcement learning for identification and control of an autonomous blimp. In *IEEE International Conference on Robotics and Automation (ICRA)*, pp. 742–747, 2007.

J. Kocijan, R. Murray-Smith, C. E. Rasmussen, and A. Girard. Gaussian process model based predictive control. In *IEEE American Control Conference*, volume 3, pp. 2214–2219, 2004.

Ilya Kostrikov. Pytorch implementations of reinforcement learning algorithms. `https://github.com/ikostrikov/pytorch-a2c-ppo-acktr`, 2018.

Ian Lenz, Ross A Knepper, and Ashutosh Saxena. Deepmpc: Learning deep latent features for model predictive control. In *Robotics: Science and Systems*, 2015.

Sergey Levine, Chelsea Finn, Trevor Darrell, and Pieter Abbeel. End-to-end training of deep visuomotor policies. *The Journal of Machine Learning Research*, 17(1):1334–1373, 2016.

Timothy P. Lillicrap, Jonathan J. Hunt, Alexander Pritzel, Nicolas Heess, Tom Erez, Yuval Tassa, David Silver, and Daan Wierstra. Continuous control with deep reinforcement learning. *CoRR*, abs/1509.02971, 2015.

David Q Mayne and Hannah Michalska. Receding horizon control of nonlinear systems. *IEEE Transactions on automatic control*, 35(7):814–824, 1990.

W Thomas Miller, Robert P Hewes, Filson H Glanz, and L Gordon Kraft. Real-time dynamic control of an industrial manipulator using a neural network-based learning controller. *IEEE Transactions on Robotics and Automation*, 6(1):1–9, 1990.

Anusha Nagabandi, Gregory Kahn, Ronald S Fearing, and Sergey Levine. Neural network dynamics for model-based deep reinforcement learning with model-free fine-tuning. *arXiv preprint arXiv:1708.02596*, 2017.

Vitchyr Pong, Shixiang Gu, Murtaza Dalal, and Sergey Levine. Temporal difference models: Model-free deep rl for model-based control. *CoRR*, abs/1802.09081, 2018.

Sashank J Reddi, Satyen Kale, and Sanjiv Kumar. On the convergence of adam and beyond. 2018.

J. Schmidhuber. An on-line algorithm for dynamic reinforcement learning and planning in reactive environments. In *Proc. IEEE/INNS International Joint Conference on Neural Networks*, pp. 253–258, 1990.

John Schulman, Filip Wolski, Prafulla Dhariwal, Alec Radford, and Oleg Klimov. Proximal policy optimization algorithms. *arXiv preprint arXiv:1707.06347*, 2017.

David Silver, Hado van Hasselt, Matteo Hessel, Tom Schaul, Arthur Guez, Tim Harley, Gabriel Dulac-Arnold, David Reichert, Neil Rabinowitz, Andre Barreto, et al. The predictron: End-to-end learning and planning. *arXiv preprint arXiv:1612.08810*, 2016.

A. Srinivas, A. Jabri, P. Abbeel, S. Levine, and C. Finn. Universal planning networks. *arXiv 1804.00645*, 2018.

Richard S Sutton. Integrated architectures for learning, planning, and reacting based on approximating dynamic programming. In *Machine Learning Proceedings 1990*, pp. 216–224. Elsevier, 1990.

Emanuel Todorov and Weiwei Li. A generalized iterative lqg method for locally-optimal feedback control of constrained nonlinear stochastic systems. In *American Control Conference, 2005. Proceedings of the 2005*, pp. 300–306. IEEE, 2005.

Emanuel Todorov, Tom Erez, and Yuval Tassa. Mujoco: A physics engine for model-based control. *2012 IEEE/RSJ International Conference on Intelligent Robots and Systems*, pp. 5026–5033, 2012.

George E Uhlenbeck and Leonard S Ornstein. On the theory of the brownian motion. *Physical review*, 36(5):823, 1930.

Niklas Wahlström, Thomas B Schön, and Marc Peter Deisenroth. From pixels to torques: Policy learning with deep dynamical models. *arXiv preprint arXiv:1502.02251*, 2015.

Manuel Watter, Jost Tobias Springenberg, Joschka Boedecker, and Martin A. Riedmiller. Embed to control: A locally linear latent dynamics model for control from raw images. In *NIPS*, 2015.

Théophane Weber, Sébastien Racanière, David P Reichert, Lars Buesing, Arthur Guez, Danilo Jimenez Rezende, Adria Puigdomenech Badia, Oriol Vinyals, Nicolas Heess, Yujia Li, et al. Imagination-augmented agents for deep reinforcement learning. *arXiv preprint arXiv:1707.06203*, 2017.